Eternal Youth, the Fate of Developing Arabidopsis Leaves upon *Rhodococcus fascians* Infection[1][C][W][OA]

Stephen Depuydt, Lieven De Veylder, Marcelle Holsters*, and Danny Vereecke

Department of Plant Systems Biology, Flanders Institute for Biotechnology, and Department of Plant Biotechnology and Genetics, Ghent University, 9052 Ghent, Belgium

The phytopathogenic actinomycete *Rhodococcus fascians* induces neoplastic shooty outgrowths on infected hosts. Upon *R. fascians* infection of Arabidopsis (*Arabidopsis thaliana*), leaves are formed with small narrow lamina and serrated margins. These symptomatic leaves exhibit reduced tissue differentiation, display more but smaller cells that do not endoreduplicate, and accumulate in the G1 phase of the cell cycle. Together, these features imply that leaf growth occurs primarily through mitotic cell division and not via cell expansion. Molecular analysis revealed that cell cycle gene expression is activated continuously throughout symptomatic leaf development, ensuring persistent mitotic cycling and inhibition of cell cycle exit. The transition at the two major cell cycle checkpoints is stimulated as a direct consequence of the *R. fascians* signals. The extremely reduced phenotypical response of a *cyclind3;1-3* triple knockout mutant indicates that the D-type cyclin/retinoblastoma/E2F transcription factor pathway, as a major mediator of cell growth and cell cycle progression, plays a key role in symptom development and is instrumental for the sustained G1-to-S and G2-to-M transitions during symptomatic leaf growth.

The Gram-positive phytopathogenic bacterium *Rhodococcus fascians* secretes growth-modulating hormones, such as cytokinins and auxins, and typically induces neoplastic, shooty outgrowths on a wide range of plant hosts (Goethals et al., 2001; Putnam and Miller, 2007). Whereas the role of auxin production in the symptomatology remains to be determined (Vandeputte et al., 2005), the central position of cytokinin secretion has been clearly established (Crespi et al., 1992, 1994; Temmerman et al., 2000; Pertry et al., 2009). The proliferation of shooty tissue in tobacco (*Nicotiana tabacum*) not only relies on activation of existing (dormant) meristems but also on de novo meristem formation in cortical tissues by reactivation of the cell cycle, a process that is accompanied by expression of the cyclins *CYCB1;1* and *CYCD3;2* (de O Manes et al., 2001). In Arabidopsis (*Arabidopsis thaliana*), only newly formed organs become symptomatic upon *R. fascians* infection. A strong induction of *CYCA2;1* expression, followed by an enhanced transcription of *CYCB1;1* and the cyclin-dependent kinase *CDKA;1* upon infection, illustrates activation of the cell cycle in this host (Vereecke et al., 2000).

Plants can rapidly alter their growth rate and pattern in response to developmental and external conditions (Traas et al., 1998; Gendreau et al., 1999). During organ formation, primordium growth is initially driven by cell proliferation, whereas the second growth phase is primarily attributed to postmitotic cell expansion of the differentiating cells through endoreduplication and vacuolization (Donnelly et al., 1999; den Boer and Murray, 2000; Nath et al., 2003). Usually, ploidy levels and cell size are positively correlated, indicating that cell expansion and differentiation depend on the endocycle (Cionini et al., 1983; Melaragno et al., 1993; Gendreau et al., 1998; Joubès et al., 1999; Beemster et al., 2003; Tsukaya, 2006), but ploidy-independent growth mechanisms also exist (De Veylder et al., 2001; Beemster et al., 2002; Jasinski et al., 2002; Schnittger et al., 2003; Ferjani et al., 2007).

Cell cycle control and plant development are mainly integrated at the cell cycle checkpoints (G1/S and G2/M) and the molecular machineries involved (De Veylder et al., 2003; Inzé, 2005; Inzé and De Veylder, 2006). G1-to-S transition and S phase progression are controlled by a D-type cyclin/retinoblastoma-related (RBR)/E2F-DP transcription factor-mediated pathway (De Veylder et al., 2002; Kosugi and Ohashi, 2003; Boudolf et al., 2004b; Magyar et al., 2005; del Pozo et al., 2006). D-type cyclins have been proposed to be the primary sensors for external conditions (Dewitte and Murray, 2003), determining the cellular commitment to the mitotic cell cycle in response to several plant growth factors, such as cytokinin, auxin, gibberellin, brassinosteroid, and Suc (Soni et al., 1995; Riou-Khamlichi et al.,

[1] This work was supported by the Bijzonder Onderzoeksfonds of Ghent University (predoctoral fellowship to S.D.).

* Corresponding author; e-mail marcelle.holsters@psb.ugent.be.

The author responsible for distribution of materials integral to the findings presented in this article in accordance with the policy described in the Instructions for Authors (www.plantphysiol.org) is: Danny Vereecke (danny.vereecke@psb.ugent.be).

[C] Some figures in this article are displayed in color online but in black and white in the print edition.

[W] The online version of this article contains Web-only data.

[OA] Open Access articles can be viewed online without a subscription.

www.plantphysiol.org/cgi/doi/10.1104/pp.108.131797

1999, 2000; Hu et al., 2000; Stals and Inzé, 2001; Oakenfull et al., 2002). Progression at the G2-to-M transition is mediated by the M phase-specific CDKs. CDKB1 is a plant-specific CDK dedicated to the G2-to-M transition (Boudolf et al., 2004b), whereas CDKA functions during both mitosis and the endocycle (Hemerly et al., 1995; Leiva-Neto et al., 2004; Verkest et al., 2005). Cell cycle exit and endoreduplication onset are accomplished through down-regulation of the mitotic CDK activity by inhibitors, such as KIP-related proteins (Wang et al., 1998; De Veylder et al., 2001; Verkest et al., 2005; Weinl et al., 2005; Nakai et al., 2006; Pettkó-Szandtner et al., 2006) and SIAMESE (SIM; Churchman et al., 2006). Other important control mechanisms for CDK activity are regulation of cyclin transcription and stability, and proteolysis by the anaphase-promoting complex-activating protein CELL CYCLE SWITCH52A (CCS52A; den Boer and Murray, 2000; Dewitte et al., 2003; Kondorosi and Kondorosi, 2004; Imai et al., 2006). Recently, in Arabidopsis, E2Fe/DEL1, a member of the E2F transcription factors present exclusively in mitotic cells, has been shown to repress the CCS52A2 activity, preventing cells from engaging in the endoreduplication program (Vlieghe et al., 2005; Lammens et al., 2008).

Here, we analyzed the development of newly formed symptomatic leaves in Arabidopsis upon infection with *R. fascians* and asked how modulation of the plant cell cycle is involved in symptom establishment. Our data show that the bacterial signals directly stimulate progression at the G1/S and G2/M checkpoints, which commits the leaf cells to mitotic cycling. Consequently, symptomatic leaves never reach maturity and are blocked in a physiological state that is relevant for niche establishment.

RESULTS

R. fascians Infection Inhibits Leaf Differentiation

Typically, infection of Arabidopsis plants with the wild-type *R. fascians* strain D188 generates symptomatic leaves with small and narrow leaf blades and strongly serrated margins (Depuydt et al., 2008). To evaluate the leaf phenotype in greater detail, the youngest nonsymptomatic leaf (leaf 7) was compared with the first symptomatic leaf (leaf 8) of plants that were infected at developmental stage 1.05, when five leaves are visible (Boyes et al., 2001). Throughout this study, infections with the virulent strain D188 were compared with control infections with its nonvirulent linear plasmid-free derivative D188-5. At 28 d postinfection (dpi), the leaf surface area, the total cell number, the cell size of the pavement cells, and the stomatal index of the abaxial epidermis were quantified. Although the leaf surface area, the total cell number, and the average cell size for leaf 7 were somewhat smaller for plants infected with the virulent strain D188, these differences were not statistically significant at the time point of analysis (Fig. 1). By contrast, leaf 8 was 4-fold smaller due to an almost 5-fold reduced cell size (Fig. 1, A–C), but there were 2- to 3-fold more cells compared with the controls (Fig. 1, A and D). Moreover, the epidermal

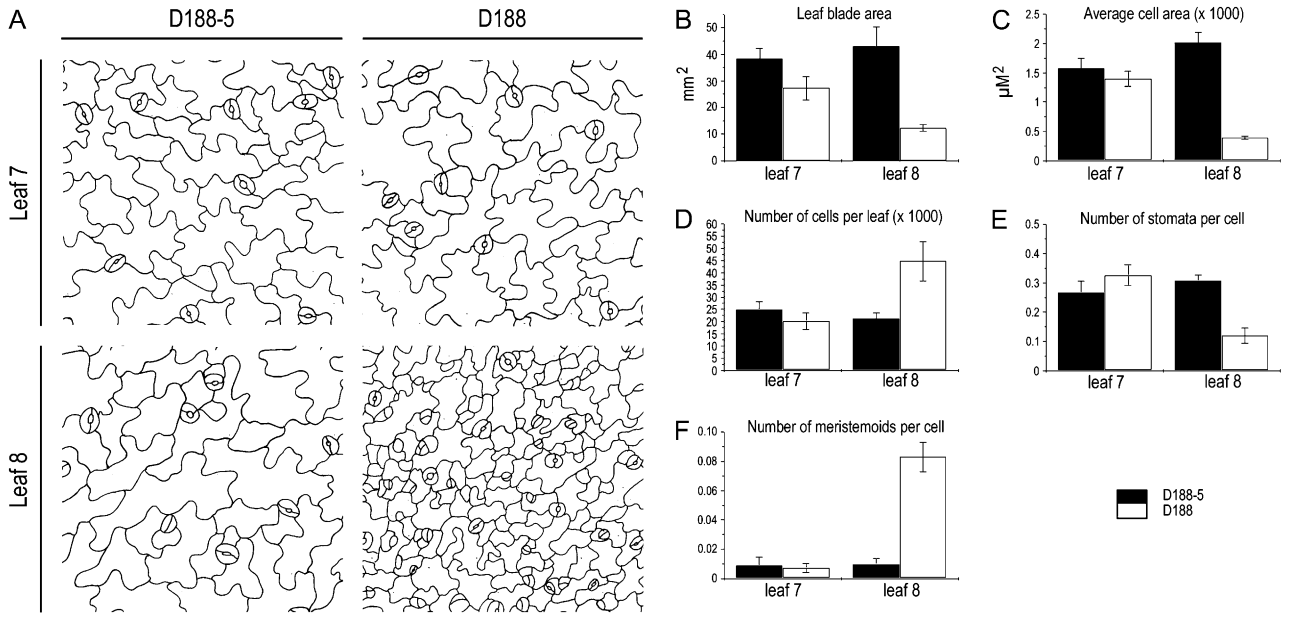

Figure 1. Epidermal pavement cell analysis of leaves 7 and 8 upon infection with *R. fascians* strain D188-5 (control) and D188. A, Drawing tube images. B, Leaf blade area. C, Average cell size. D, Total number of cells per leaf. E, Number of stomata per cell. F, Number of meristemoids per cell. All analyses were done at 28 dpi ($n = 5$). Error bars represent SE.

pavement cells of the responsive leaves did not have the typical sinusoid outline but remained rather polygon shaped (Fig. 1A). The stomatal index was lower in symptomatic leaves (Fig. 1E), but more meristemoids, the stomatal precursor cells, occurred per cell than in control infections (Fig. 1F).

Altogether, these observations suggest that cell proliferation is the dominant mechanism for growth in symptomatic leaves and that differentiation is impaired. The latter was confirmed by microscopic analysis of cross-sections through the lamina (Fig. 2, A and B). Indeed, all of the parenchyma cells of D188-infected leaves were spherical with fewer intercellular air spaces than in control leaves, making it difficult to distinguish the palisade and spongy mesophyll layers (Fig. 2).

R. fascians Prevents Endocycling during Leaf Development

The data above indicate that the balance between cell proliferation and cell differentiation is disturbed during leaf maturation upon infection with *R. fascians* strain D188. In a time course experiment, we examined the endoreduplication kinetics as a marker for cell differentiation. Infections were carried out as described above, and together with leaf 5, the next three emerging leaves were analyzed at 3, 7, 10, 14, 16, 19, and 24 dpi (Fig. 3). Hence, four different stages in leaf development were considered: outgrowing primordia and young, expanding, and mature leaves. For leaves 5 and 6, no significant differences between the two conditions were measured, which was anticipated because of the lack of morphological alterations in these leaves (Depuydt et al., 2008). In leaf 7, the increase in cells with an 8C content started later upon D188 infection, suggesting a delay in the endoreduplication onset that possibly correlated with the moderate leaf phenotype (Fig. 1). Strikingly, throughout the experiment, the ploidy levels of leaf 8 did not change. Since the cell numbers strongly increased, this observation does not reflect a cell cycle stop but rather indicates that endoreduplication did not occur, confirming that growth of symptomatic leaves is driven by proliferative divisions and not by expansion via endoreduplication.

Maintenance of High Transcription Levels of Mitotic Cell Cycle Genes throughout Symptomatic Leaf Development Imposes a Commitment to Mitotic Cycling

Most cells (60%–65%) in symptomatic leaves have a 2C content, implying that infection with *R. fascians* promotes the G2-to-M transition. Since *CDKB1;1* expression typically correlates with proliferating cells and plays a key role at the G2/M checkpoint, the expression pattern of *CDKB1;1* was analyzed upon infection with *R. fascians*. Histochemical analyses of *CDKB1;1*:*GUS* marker lines revealed promoter activity throughout the lamina of symptomatic leaves. The reported typical stomatal expression (Boudolf et al., 2004a) was higher than that in control leaves (Fig. 4, A–C). Quantitative reverse transcription (qRT)-PCR of the *CDKB1;1* transcript level over 2 weeks showed a progressive decrease as the control leaf 8 matured and started to endoreduplicate (Fig. 4D). In contrast, upon D188 infection, *CDKB1;1* expression in leaf 8 initially remained constant and after 16 dpi it increased drastically (Fig. 4D). The significance of this high *CDKB1;1* expression upon D188 infection was illustrated by the complete phenotypical responsiveness of a CDKB1;1.N161 line, in which a dominant negative allele of *CDKB1;1* is expressed, resulting in decreased CDK activity and increased ploidy levels (Boudolf et al., 2004b; Fig. 4, E and F). The typically high proportion of cells with a 2C content upon infection suggests that the continuous activation of the transcription of the wild-type allele in this mutant background largely compensates for the negative effect of the mutant allele. The latter was not com-

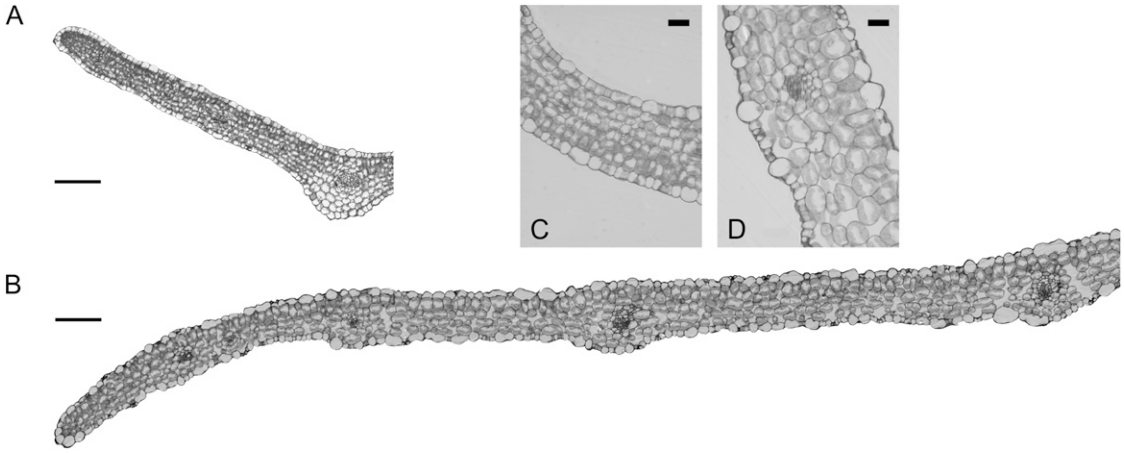

Figure 2. Central cross-sections and close-ups through a *R. fascians* D188- (A and C) and a D188-5-infected leaf (B and D) at 28 dpi. Bars = 60 μm (A and B) and 20 μm (C and D).

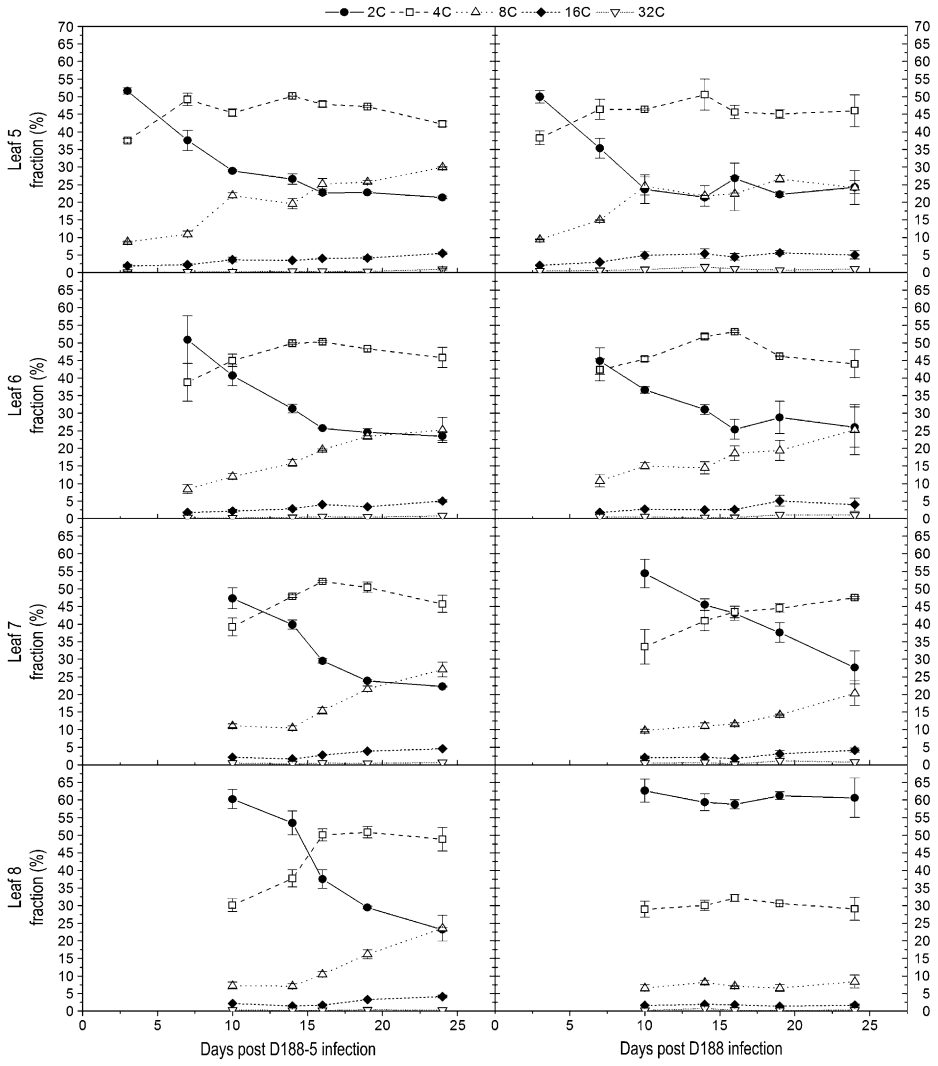

Figure 3. DNA ploidy level distribution of leaves 5, 6, 7, and 8 upon infection with *R. fascians* D188-5 (left) and D188 (right). The data represent averages of two independent biological repeats with two technical replicates each. The error bars depict SD.

pletely overruled, however, because the 2C content was 15% lower than that of infected wild-type plants (Fig. 4, E and F).

Expression of *CDKA;1* and *CYCA2;3*, as a complex involved in the negative regulation of endocycling (Imai et al., 2006), was also specifically down-regulated as control leaves differentiated (Fig. 5, A and B). Interestingly, upon infection with D188, a biphasic expression pattern reminiscent of that of *CDKB1;1* was observed for both genes (Fig. 5, A and B), confirming the proliferative status of symptomatic leaves. A similar differential expression in control versus infected leaves of *E2Fe/DEL1* (Fig. 5C), exclusively present in mitotically dividing cells (Vlieghe et al., 2005; Lammens et al., 2008), together with the expansion of the expression zone in infected *E2Fe/DEL1*:*GUS* leaves beyond the leaf base into the leaf blade (Fig. 5, D and E), further support that leaf growth is only driven by mitotic cell divisions upon *R. fascians* infection.

Infection and subsequent determination of the disease phenotype and ploidy level distribution in symptomatic leaves of *ccs52a2* and *del1-1* knockout plants and in plants overexpressing *E2Fe/DEL1* or *SIM* showed that these regulators do not play a significant role in the increased CDK activity and the stimulated progression at the G2-to-M transition during symptom development (Supplemental Fig. S1), suggesting that CDK expression and/or activity might be directly targeted by the *R. fascians* signals.

R. fascians Infection Recruits the CYCD3/RBR Pathway to Stimulate G1-to-S Transition and to Promote Proliferation over Differentiation

The continuation of mitotic cell divisions during symptomatic leaf development implies that cells not only efficiently pass the G2-to-M transition but subsequently cross the G1/S checkpoint and enter the S phase of the cell cycle. Entry into the S phase involves RBR phosphorylation and subsequent activation of S-phase gene expression in a *CYCD3*-dependent way (De Veylder et al., 2002; Dewitte et al., 2003). Although

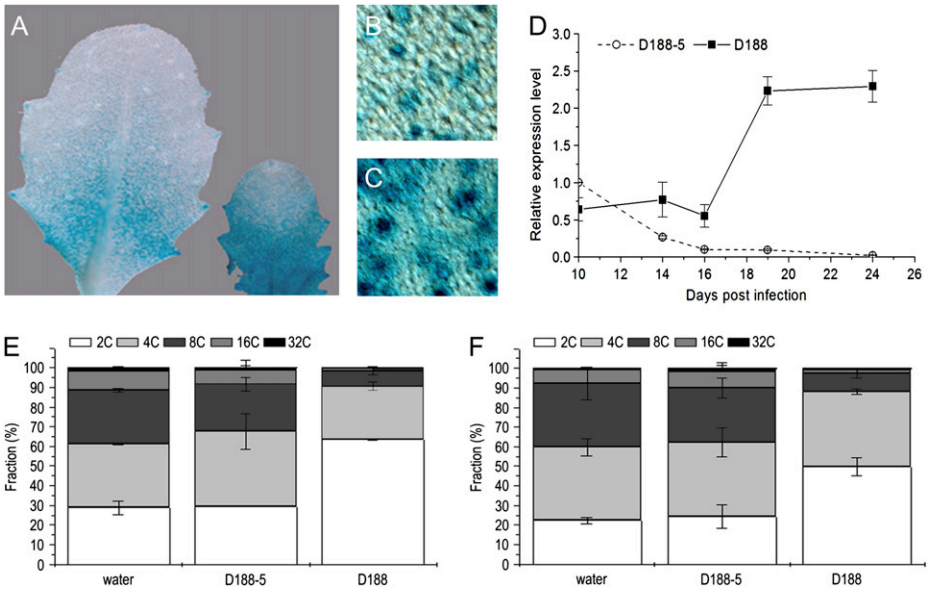

Figure 4. Role of CDKB1;1 in the stimulated G2-to-M transitions upon *R. fascians* infection. A, *CDKB1;1*:*GUS* expression in a young developing leaf of a control plant (left) and a *R. fascians* D188-infected plant (right). B and C, *CDKB1;1*:*GUS* expression at the cellular level in stomata of control and D188-infected leaves, respectively. D, Time course expression profile of *CDKB1;1* upon infection. E and F, DNA ploidy level distribution of the Col-0 wild type and of CDKB1;1.N161 in control plants and upon infection at 24 dpi, respectively.

RBR activity is mainly controlled at the posttranscriptional level, transcription of *RBR* was on average 2-fold lower upon infection with strain D188 than that of controls (Table I), suggesting that G1-to-S transition is modulated during symptom development. Interestingly, the small size of epidermal pavement cells, their polygonic shape, the reduced tissue differentiation, and the prevention of endoreduplication in symptomatic leaves nearly phenocopy the leaf phenotype of transgenic *CYCD3;1*-overexpressing (*CYCD3;1*^{OE}) Arabidopsis plants (Dewitte et al., 2003). Nevertheless, while leaf expansion was compromised upon D188 infection, this is not the case in the *CYCD3;1*^{OE} plants under the tested conditions. The expression of all three *CYCD3* genes of Arabidopsis was down-regulated as control leaves matured, but their expression during symptomatic leaf development exhibited the typical biphasic pattern, albeit with different kinetics. *CYCD3;1* responded first (the differential expression started between 4 and 7 dpi when assayed on complete shoot tissue [data not shown]) and was up-regulated 4-fold at the end of the experiment (Fig. 6A). *CYCD3;2* up-regulation only started between 10 and 14 dpi, but the final expression level was 10-fold higher than the control level (Fig. 6B). Finally, *CYCD3;3* expression responded last and reached a 6-fold higher level than that of the control (Fig. 6C). Histochemical analysis confirmed the up-regulation of all three genes and showed that the expression zone in the leaf was not extended upon infection (Fig. 6, D–I).

These data suggested that the CYCD3/RBR/E2F-DP pathway might be modulated upon *R. fascians* infection by direct targeting of the *CYCD3* genes. The strongly reduced response of a *cycd3;1-3* triple mutant line confirmed this hypothesis (Table I; Fig. 7). Importantly, in the triple mutant, the most typical aspects of the symptomatology were much less pronounced: activation of axillary meristems was only observed in 7% of the infected plants (versus 67% in wild-type plants), and leaves with serrated margins were not observed (versus 95% in wild-type plants). Leaf expansion was impaired upon infection, but not to the same extent as in infected wild-type plants (Fig. 7). The epidermal pavement cells of the infected triple mutant were sinusoid rather than polygon shaped, and their size was intermediate between the *cycd3;1-3* controls and infected wild-type plants (Fig. 7). Flow cytometric analysis during development of leaf 8 of the noninfected *cycd3;1-3* triple mutant revealed an initially higher level of cells with a 4C content and an earlier and steeper increase of cells with an 8C content (Fig. 8A) than in noninfected wild-type leaves (Fig. 3), confirming the premature onset of endoreduplication (Dewitte et al., 2007). In contrast to the effect on wild-type plants (Fig. 3), infection with D188 did not result in the typically high proportion of cells with a 2C content during development of leaf 8 of the *cycd3;1-3* mutant, indicating that the activation of *CYCD3* expression upon infection is required for the preclusion of endocycle onset. Interestingly, the number of cells with an 8C content decreased over time and was finally half that of the controls, suggesting that the *R. fascians* signals can still interfere with endoreduplication in the *cycd3;1-3* mutant plants. The intermediate response of *cycd3;1-3* plants to *R. fascians* infection could also be demonstrated at the molecular level by assessing the expression of marker genes (Depuydt et al., 2008). In agreement with the absence of leaf margin serrations, no ectopic expression of *SHOOT MERISTEMLESS* (*STM*), a meristem-associated class I *KNOX* gene, could be observed (Table I), but cytokinin signaling was still activated, as indicated by enhanced

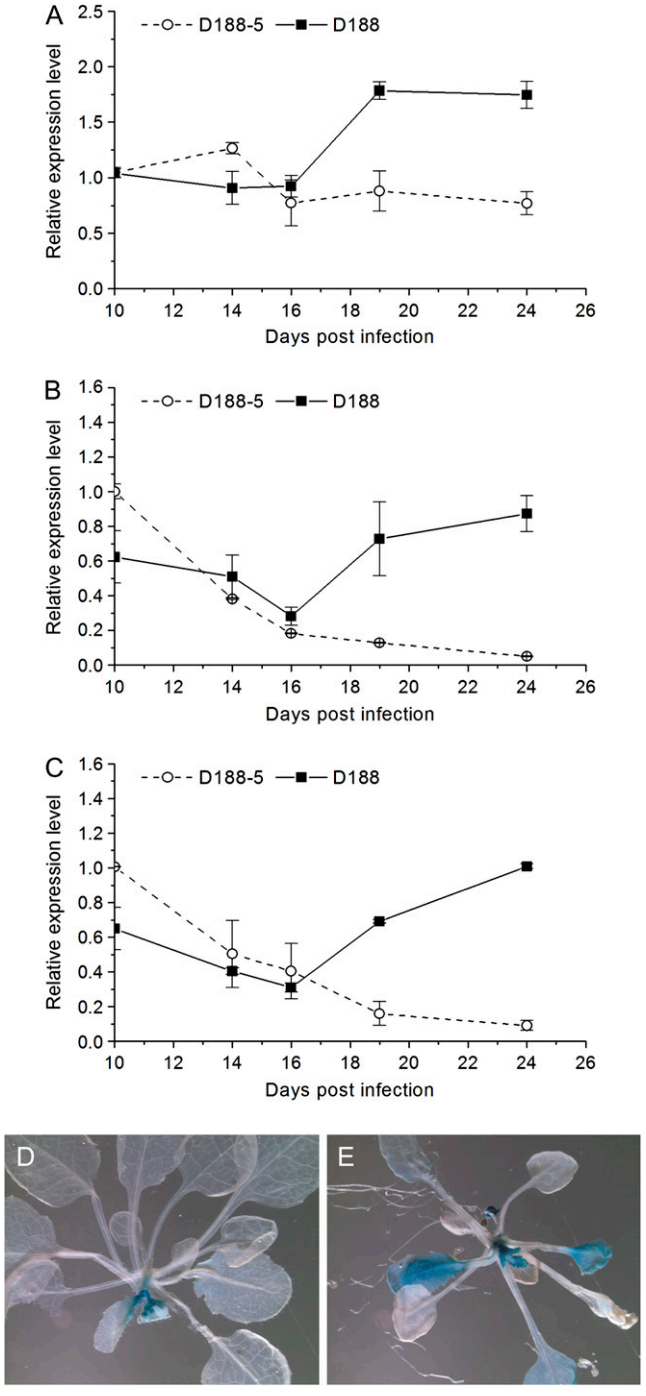

Figure 5. Assessment of the role of endocycle regulators during symptomatic leaf development. A to C, Expression kinetics of *CDKA;1* (A), *CYCA2;3* (B), and *E2Fe/DEL1* (C) in leaf 8 upon infection. D and E, *E2Fe/DEL1*:*GUS* plants after infection with *R. fascians* D188-5 and strain D188, respectively.

ARABIDOPSIS RESPONSE REGULATOR5 (*ARR5*) expression. Moreover, induced expression of *E2Fe/DEL1* and *CDKB1;1* and down-regulation of *RBR* were maintained in the infected *cycd3;1-3* triple mutants. Nevertheless, the differential expression levels were much lower than those of infected wild-type controls (Table I).

As described above, *CYCD3;1*^{OE} plants had features that resembled *R. fascians*-induced phenotypes. Interestingly, these transgenic lines were only partially responsive to infection. Whereas axillary meristems were activated as in wild-type plants, leaf expansion was only partially compromised, no leaf serrations were observed (Fig. 7A), and the very small epidermal pavement cell size of the *CYCD3;1*^{OE} plants was not further reduced upon infection (Fig. 7B). Moreover, the DNA ploidy level distribution did not change upon infection, no high population of cells with a 2C content could be established (Fig. 8D), and no differential expression of the marker genes was detected (Table I).

DISCUSSION

Arabidopsis leaves that develop upon infection with *R. fascians* strain D188 have a typical small and narrow leaf blade and serrated margins. The latter is accomplished by ectopic expression of meristem-associated class I *KNOX* genes, but the cause for the strongly reduced leaf expansion had not been addressed (Depuydt et al., 2008). Here, we determined that the small lamina size is caused by an almost 5-fold reduction in cell size that could not be compensated for by the 2- to 3-fold increase in cell number. The increased number of meristemoids, the reduced tissue differentiation, and the very high level of cells with a 2C content all illustrate that cells in D188-infected leaves hardly differentiate and remain in the proliferative state. These data imply that the time window in which mitotic cell division drives leaf growth is greatly extended upon infection and, moreover, indicate that, in symptomatic leaves, the subsequent stage of leaf growth via cell expansion, driven by endoreduplication, is never attained.

An increase in cell cycle gene expression upon infection with *R. fascians* had been reported previously in tobacco and Arabidopsis plants. Outer cortical cells of infected tobacco plants reenter the cell cycle, and subsequent divisions result in the formation of shoot primordia. The reiteration of this process together with the activation of axillary meristems ultimately culminates in the typical leafy gall symptom on tobacco and is correlated with the up-regulation of *CYCD3;2* and *CYCB1;1* (de O Manes et al., 2001). Also in Arabidopsis, activation of axillary meristems and de novo meristem formation contribute to symptom development (de O Manes et al., 2004; Simón-Mateo et al., 2006) and are associated with elevated expression of *CYCA2;1*, *CYCB1;1*, and *CDKA;1* (Vereecke et al., 2000). Here, with the developing Arabidopsis leaf as a model system, we found that during infected leaf development the transcriptional profiles of the tested cell cycle genes all showed a typically biphasic pattern: initial expression was mostly constitutive but increased steadily from 16 dpi onward. In contrast, in control leaves, during maturation, the expression of the tested

Table I. *Phenotypical and molecular alterations in Col-0, Ler, cycd3;1-3, and CYCD3;1^{OE} upon R. fascians D188 infection*

Col-0, Columbia; L*er*, Landsberg *erecta*; ++, strong response; +, intermediate response; (+), weak response; −, no response.

Phenotypic Trait	Col-0/L*er*	*cycd3;1-3*	*CYCD3;1^{OE}*
Anthocyanin production	++	+	+
Pale color	+	−	+
Small, newly formed leaves	++	+	++
Serrated margins of newly formed leaves	++	−	−
Activation of axillary meristems	++	(+)	+
Flowering induction	+	+	+
Inhibited elongation of flower stalks	+	+	+
Endoreduplication upon D188 infection	−	(+)	−
Expression in leaf tissue: fold changes at 24 dpi (*R. fascians* D188 versus D188-5 infection)			
STM	>1,000[a]	1	1
ARR5	>12[a]	2.69	0.40
E2Fe/DEL1	10	1.73	1
RBR	0.52	0.46	1
CDKB1;1	20	2.39	0.66

[a]Data derived from Depuydt et al. (2008).

cell cycle genes steadily declined. Interestingly, at 16 dpi, the sampled leaf is approximately 8 d old, the age at which the switch from mitotic cycling to endocycling occurs in control leaves (Beemster et al., 2002). Consequently, the data suggest that already at the early stages of leaf development, infection activates the cell cycle. However, instead of a developmental switch into endocycling, proliferative cell division is strongly stimulated in infected leaves, representing the single mode of organ growth.

The persistent expression of the mitotic CDKs, *CDKB1;1* and *CDKA;1*, and of *CYCA2;3* continues to promote the G2-to-M transition. A fast progression through mitosis had been observed in tobacco Bright

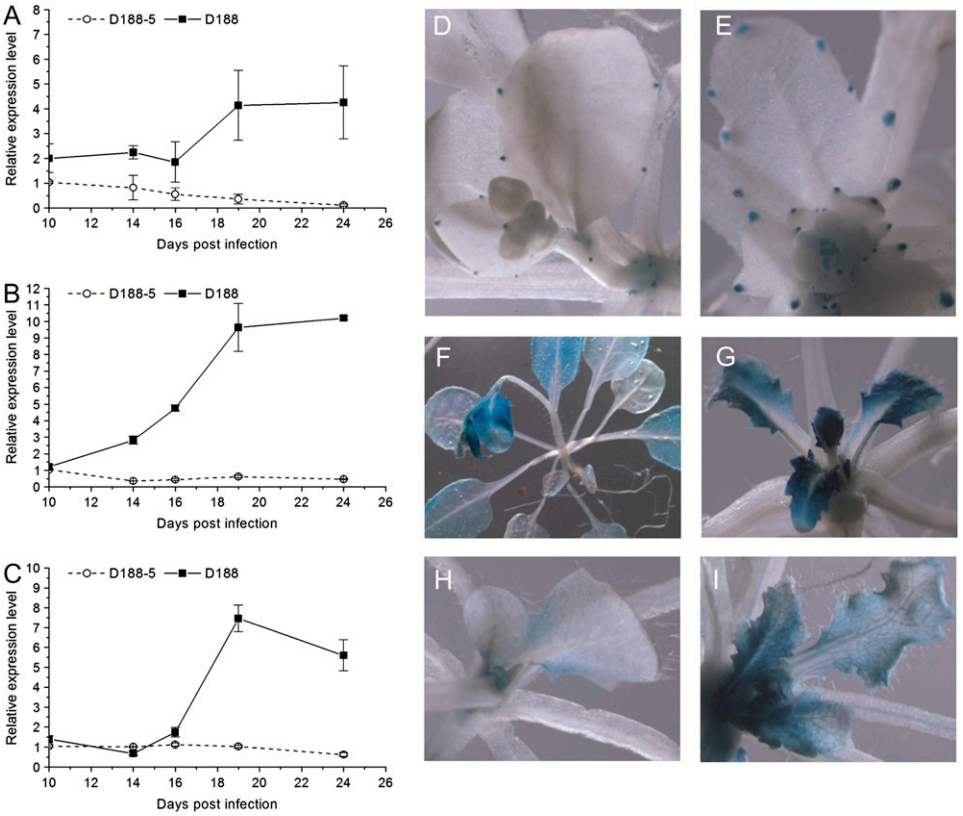

Figure 6. *CYCD3* expression during *R. fascians* symptomatology. A to C, Expression kinetics of *CYCD3;1* (A), *CYCD3;2* (B), and *CYCD3;3* (C) in leaf 8 upon infection with *R. fascians* strains D188-5 and D188. D to I, Histochemical localization of *CYCD3;1* (D and E), *CYCD3;2* (F and G), and *CYCD3;3* (H and I) upon *R. fascians* D188-5 (D, F, and H) and D188 (E, G, and I) infection at 24 dpi.

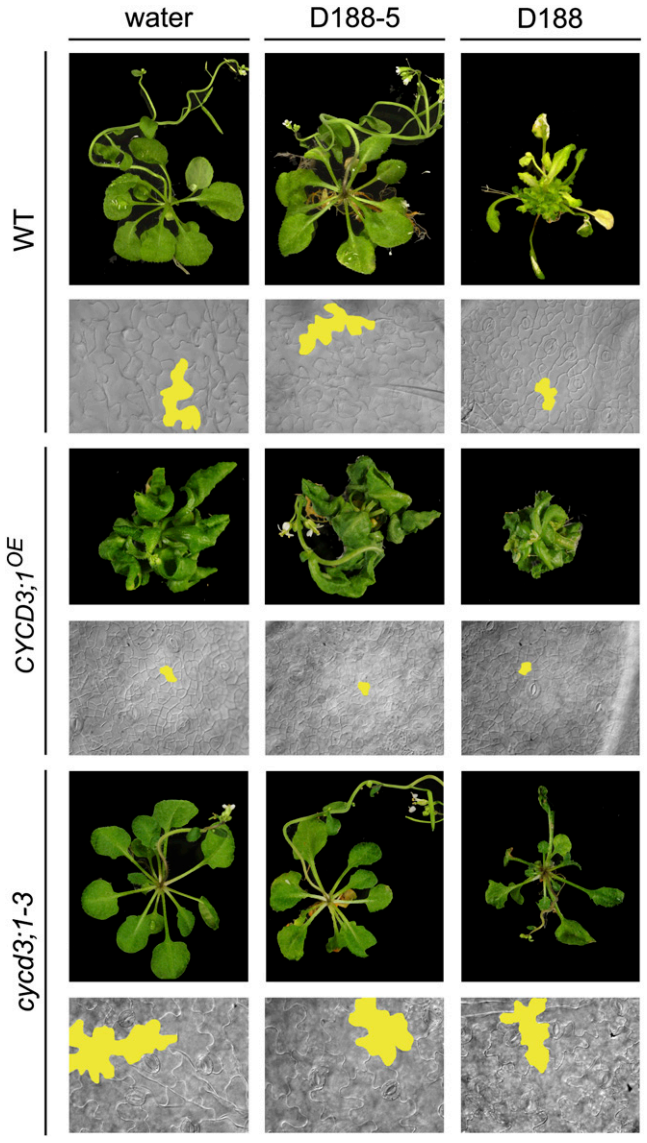

Figure 7. Functional analysis of the involvement of *CYCD3* during *R. fascians* symptomatology. Complete plant phenotypes and epidermal pavement cell size of wild type (WT), *CYCD3;1*^{OE} (L*er* background), and *cycd3;1-3* (Col-0 background) plants upon infection. As the wild type, Col-0 is shown; L*er* behaved similarly upon infection (data not shown).

Yellow 2 cell cultures infected with *R. fascians* that was accompanied with transcriptional activation of genes associated with the G2/M phase (Vandeputte et al., 2007). Interestingly, CDKB1;1.N161 plants, expressing a dominant negative version of *CDKB1;1*, were phenotypically fully responsive, suggesting that in infected plants, the induced expression of the wild-type *CDKB1;1* allele was sufficiently high to overcome the negative effect of the mutant allele. Expression of *E2Fe/DEL1*, an indirect activator of CDKB1;1 activity, was induced upon infection, but functional analysis revealed that the E2Fe/DEL1/CCS52A2 pathway was not involved in the increased CDK activity. Altogether, these data support the role of CDKB1;1 in the progression over the G2/M checkpoint during the *R. fascians*-induced pathology and imply that *CDKB1;1* is possibly a direct target for the *R. fascians* signals. The main virulence factors of *R. fascians* are the *fas*-encoded cytokinins (Crespi et al., 1992, 1994; Vereecke et al., 2000; Pertry et al., 2009). Because cytokinins are known to directly regulate cell division at the G2-to-M transition by dephosphorylating CDKs (Zhang et al., 1996, 2005; Laureys et al., 1998; Spíchal et al., 2007), besides stimulating *CDKB1;1* expression, the direct activation of CDKs by the bacterial cytokinins might represent a second level of stimulation at the G2/M checkpoint.

The transcriptional analysis indicated that the CYCD3/RBR/E2F-DP pathway that controls the G1-to-S transition was also modulated. Indeed, *RBR* expression was down-regulated upon infection, and all three *CYCD3* genes were significantly up-regulated throughout development of the infected leaves. The CYCD3 proteins function as growth factor sensors (Riou-Khamlichi et al., 1999; Sorrell et al., 1999; Francis and Sorrell, 2001; Stals and Inzé, 2001), so the transcriptional induction by the bacterial cytokinins is probably directly responsible for the promotion of the G1-to-S transition. Importantly, a *cycd3;1-3* triple knockout mutant had a strongly reduced response toward infection. Infected plants were overall smaller, leaf expansion was partially impaired, and epidermal pavement cell size was reduced, but strikingly, the typical serrations of the leaf margins and the activation of axillary meristems were nearly absent and the characteristic ploidy level distribution was not attained. Moreover, the differential expression level of *STM*, *ARR5*, *E2Fe/DEL1*, *RBR*, and *CDKB1;1*, used as marker genes, was much lower than that of infected wild-type plants. The loss of function of all three *CYCD3* genes did not prevent the development into adult plants; therefore, CYCD3 is not essential for mitosis or morphogenesis during regular plant development but determines cell number, cell size, and endoreduplication in lateral shoot organs (Dewitte et al., 2007). Nevertheless, our data indicate that the CYCD3 proteins are instrumental for the developmental alterations that are triggered by the exogenous signals provided by *R. fascians*. Interestingly, CYCD3 has also been implicated in G2-to-M transition, because *CYCD3* transcription and CYCD3;3-associated kinase activity peak at this checkpoint (Sorrell et al., 1999; Schnittger et al., 2002). Moreover, the occurrence of an E2F/DP-binding site in the promoter of *CDKB1;1* directly places CYCD3 at the G2-to-M transition (Menges et al., 2005; Inzé and De Veylder, 2006).

Although transgenic *CYCD3;1*^{OE} plants exhibit features that are reminiscent of *R. fascians*-induced symptoms, the overall phenotype was very different from that of infected wild-type plants. Indeed, expression of *CYCD3;1* from the 35S promoter does not affect the overall organ size. More importantly, in contrast to *R. fascians*-infected plants in which cells accumulate in the G1 phase, the strongly enhanced G1-to-S transition

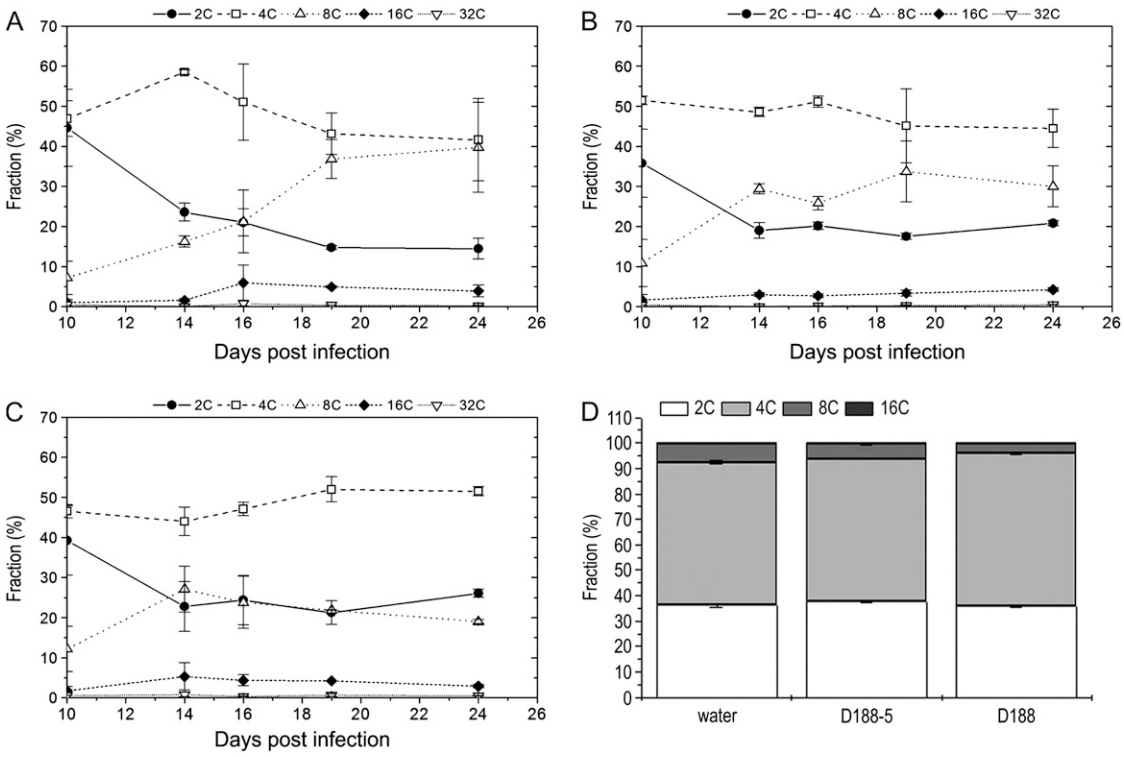

Figure 8. DNA ploidy level distribution in *cycd3;1-3* and *CYCD3;1*^{OE} plants. A to C, Leaf 8 of *cycd3;1-3* plants upon mock (A), *R. fascians* D188-5 (B), and D188 (C) infection. D, DNA ploidy level distribution of *CYCD3;1*^{OE} upon infection at 24 dpi. Error bars represent SD ($n = 4$).

is not accompanied with a promotion of the G2-to-M transition; hence, cells accumulate in the G2 phase (Dewitte et al., 2003; Menges et al., 2006). Unexpectedly, *CYCD3;1*^{OE} plants were phenotypically much less responsive to *R. fascians*, an observation supported by the lack of differential expression of the marker genes and the absence of the typical ploidy distribution. Possibly, cells in G2 phase are much less sensitive to the *R. fascians* signals, or, alternatively, in the *CYCD3;1*^{OE} plants, the leaf tissue is already pushed to its mitotic limit.

In conclusion, our data demonstrate that *R. fascians* modulates plant development by manipulating both checkpoints of the cell cycle (Fig. 9). Upon infection, the fast G1-to-S transition is accompanied by a fast G2-to-M transition; thus, most cells of symptomatic leaves are in the G1 phase. CYCD3 activity plays a central role in symptom development and potentially mediates both transitions, although direct targeting of CDKB1;1 might also contribute to the persistent mitotic cycling of the infected tissues. As a consequence of the action of the bacterial morphogens, newly formed organs only grow through mitotic cell divisions, hardly differentiate, and never reach maturity. It is hypothesized that young dividing tissues would provide the bacteria with specific nutrients that give a selective advantage over other plant-inhabiting microorganisms (Vereecke et al., 2002a, 2002b). Metabolic profiling experiments in which control and infected Arabidopsis leaves were compared indeed demonstrated that symptomatic leaves are sink tissues and represent an established niche for *R. fascians*. Importantly, the altered physiological status of infected tissues allows full manifestation of the bacterial virulence potential (Depuydt et al., 2009).

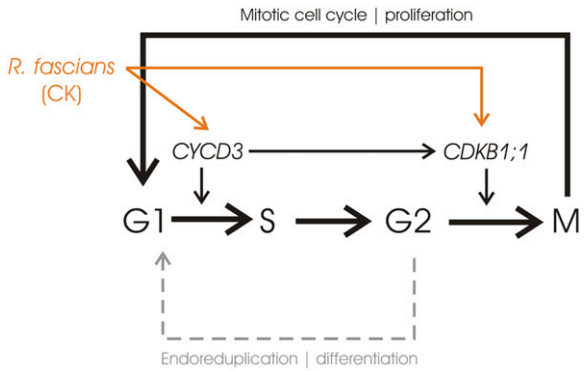

Figure 9. Schematic representation of the *R. fascians* action in disturbing the progression from cell proliferation into differentiation by manipulating the cell cycle at the G1-to-S and G2-to-M transitions, mainly via *CYCD3* and possibly directly via *CDKB1;1*. Dashed lines represent inhibited actions. CK, Cytokinin. [See online article for color version of this figure.]

MATERIALS AND METHODS

Plant Materials and Growth Conditions

Arabidopsis (*Arabidopsis thaliana* L. Heyhn.) seeds were germinated and grown on half-strength Murashige and Skoog medium in a growth chamber under a 16-h/8-h light/dark photoperiod at 21°C ± 2°C, after sterilization by submergence for 2 min in 70% ethanol (v/v) and 12 min in 5% (w/v) NaOCl supplemented with 0.1% (v/v) polyoxyethylenesorbitan 20, and rinsing at least five times with sterile water. Unless stated otherwise, wild-type ecotype C24 was used for the infection experiments, obtained from the European Arabidopsis Stock Centre. *CYCD3;1*^{OE} and *cycd3;1-3* lines were obtained from Jim Murray (Dewitte et al., 2003, 2007); *CDKB1;1.N161*, *del1-1*, *DEL1*^{OE}, *ccs52a2*, *CDKB1;1:GUS*, and *E2Fe/DEL1:GUS* were from Lieven De Veylder (Boudolf et al., 2004b; Vlieghe et al., 2005; Lammens et al., 2008); *CYCD3;1:GUS*, *CYCD3;2:GUS*, and *CYCD3;3:GUS* were from Tom Beeckman (Dewitte et al., 2007), and *SIM*^{OE} lines were from John Larkin (Churchman et al., 2006).

Bacterial Strains, Growth Conditions, and Infection

The *Rhodococcus fascians* strains used were the pathogenic strain D188, containing the linear virulence plasmid pFiD188 and its plasmid-free non-pathogenic derivative D188-5 (Desomer et al., 1988). These strains were grown in liquid yeast extract broth for 2 d at 28°C under gentle agitation until late exponential phase. Prior to infection, these cultures were washed and concentrated 4-fold by resuspension of the bacterial pellets in sterile distilled water. At 16 d after germination, Arabidopsis plants were infected at stage 1.05 (Boyes et al., 2001) by local application of a drop of bacterial culture to the shoot apical meristem.

Analysis of Leaf Growth Parameters

The leaf area was determined by photographing the leaf with a binocular MZFLIII (Leica) and analyzing the picture with the public domain image-analysis program ImageJ (http://rsb.info.nig.gov/ij/; version 1.32j). For cell density and cell area, the leaves were cleared overnight in ethanol (70% [v/v]) and stored in lactic acid for analysis on a microscope stage fitted with differential interference contrast optics (DMLB; Leica). Images of at least 30 cells of the abaxial epidermis located at 25% and 75% from the leaf base, halfway between the midrib and the leaf margin, were drawn with a drawing tube mounted on the microscope. These images were scanned and processed with ImageJ. The total number of cells was estimated by dividing the leaf area with the average cell area. At least five independent biological repeats were analyzed, and average data are shown. The total numbers of stomata and meristemoids were derived by extrapolating the number of stomata and meristemoids, identified by cell shape and size, in the drawing tube images to the full leaf surface area.

Flow Cytometric Analysis

Depending on the experiment, leaf 5, 6, 7, and/or 8 was sampled (Figs. 3 and 8, A–C) or symptomatic leaves were pooled (Figs. 4, E and F, and 8D; Supplemental Fig. S1). Leaves were chopped with a razor blade in 300 μL of buffer (45 mM $MgCl_2$, 30 mM sodium citrate, 20 mM MOPS, and 1% Triton X-100, pH 7; Galbraith et al., 1991). This mixture was filtered over a 30-μm mesh and, subsequently, 1 μL of 4,6′-diamidino-2-phenylindole from a 1 mg mL^{-1} stock was added. The nuclei were analyzed with the CyFlow flow cytometer with the accompanying FloMax software (Partec). Each sample was measured in two or three biological repeats and two technical replicates, unless stated otherwise.

Histochemical Analysis

The GUS assays were done as described (Beeckman and Engler, 1994). For microscopic analysis, samples were cleared by mounting in 90% lactic acid (Acros Organics).

qRT-PCR

For qRT-PCR, leaf 8 was sampled in a time course experiment and stored at −70°C until further processing. RNA was extracted from leaf tissue with the RNeasy kit (Qiagen). cDNA was prepared from 2 μg of total RNA with SuperScript II reverse transcriptase (Invitrogen) according to the manufacturer's instructions. qRT-PCRs were quantified on a Lightcycler480 apparatus (Roche Diagnostics) with SYBR Green for detection in a 5-μL volume (2.5 μL of master, 0.25 μL of 5 μM of each forward and reverse primer, and 2 μL of cDNA) in triplicate on a 384-multiwell plate to allow determination of mean and SD of cycle threshold (C_T) values. Data were analyzed with the $2^{-\Delta\Delta C_T}$ method (Livak and Schmittgen, 2001), and values were normalized against those of *ACTIN2*, which was used as an internal standard. The mean expression level was calculated from six replicates of two biological repeats, obtained from two independent experiments. Primer sequences are given in Supplemental Table S1.

Supplemental Data

The following materials are available in the online version of this article.

Supplemental Figure S1. DNA ploidy level distribution upon infection of *del1-1*, *DEL1*^{OE}, *ccs52a2*, and *SIM*^{OE} plants at 24 dpi.

Supplemental Table S1. Primers used in qRT-PCR amplification.

ACKNOWLEDGMENTS

We thank Gerrit Beemster for fruitful discussions, Walter Dewitte for critical reading of the manuscript, Martine De Cock for help in preparing it, and Karel Spruyt for photographs.

Received October 28, 2008; accepted December 25, 2008; published December 31, 2008.

LITERATURE CITED

Beeckman T, Engler G (1994) An easy technique for the clearing of histochemically stained plant tissue. Plant Mol Biol Rep **12:** 37–42

Beemster GTS, De Vusser K, De Tavernier E, De Bock K, Inzé D (2002) Variation in growth rate between Arabidopsis ecotypes is correlated with cell division and A-type cyclin-dependent kinase activity. Plant Physiol **129:** 854–864

Beemster GTS, Fiorani F, Inzé D (2003) Cell cycle: the key to plant growth control? Trends Plant Sci **8:** 154–158

Boudolf V, Barrôco R, de Almeida Engler J, Verkest A, Beeckman T, Naudts M, Inzé D, De Veylder L (2004a) B1-type cyclin-dependent kinases are essential for the formation of stomatal complexes in *Arabidopsis thaliana*. Plant Cell **16:** 945–955

Boudolf V, Vlieghe K, Beemster GTS, Magyar Z, Torres Acosta JA, Maes S, Van Der Schueren E, Inzé D, De Veylder L (2004b) The plant-specific cyclin-dependent kinase CDKB1;1 and transcription factor E2Fa-DPa control the balance of mitotically dividing and endoreduplicating cells in *Arabidopsis*. Plant Cell **16:** 2683–2692

Boyes DC, Zayed AM, Ascenzi R, McCaskill AJ, Hoffman NE, Davis KR, Görlach J (2001) Growth stage-based phenotypic analysis of *Arabidopsis*: a model for high throughput functional genomics in plants. Plant Cell **13:** 1499–1510

Churchman ML, Brown ML, Kato N, Kirik V, Hülskamp M, Inzé D, De Veylder L, Walker JD, Zheng Z, Oppenheimer DG, et al (2006) SIAMESE, a novel plant-specific cell cycle regulator controls endoreplication onset in *Arabidopsis thaliana*. Plant Cell **18:** 3145–3157

Cionini PG, Cavallini A, Baroncelli S, Lercari B, D'Amato F (1983) Diploidy and chromosome endoreduplication in the development of epidermal cell lines in the first foliage leaf of durum wheat (*Triticum durum* Desf.). Protoplasma **118:** 36–43

Crespi M, Messens E, Caplan AB, Van Montagu M, Desomer J (1992) Fasciation induction by the phytopathogen *Rhodococcus fascians* depends upon a linear plasmid encoding a cytokinin synthase gene. EMBO J **11:** 795–804

Crespi M, Vereecke D, Temmerman W, Van Montagu M, Desomer J (1994) The *fas* operon of *Rhodococcus fascians* encodes new genes required for efficient fasciation of host plants. J Bacteriol **176:** 2492–2501

del Pozo JC, Diaz-Trivino S, Cisneros N, Gutierrez C (2006) The balance between cell division and endoreplication depends on E2FC-DPB,

transcription factors regulated by the ubiquitin-SCF^{SKP2A} pathway in *Arabidopsis*. Plant Cell **18:** 2224–2235

den Boer BGW, Murray JAH (2000) Control of plant growth and development through manipulation of cell-cycle genes. Curr Opin Biotechnol **11:** 138–145

de O Manes C-L, Beeckman T, Ritsema T, Van Montagu M, Goethals K, Holsters M (2004) Phenotypic alterations in *Arabidopsis thaliana* plants caused by *Rhodococcus fascians* infection. J Plant Res **117:** 139–145

de O Manes C-L, Van Montagu M, Prinsen E, Goethals K, Holsters M (2001) De novo cortical cell division triggered by the phytopathogen *Rhodococcus fascians* in tobacco. Mol Plant Microbe Interact **14:** 189–195

Depuydt S, Doležal K, Van Lijsebettens M, Moritz T, Holsters M, Vereecke D (2008) Modulation of the hormone setting by *Rhodococcus fascians* results in ectopic *KNOX* activation in Arabidopsis. Plant Physiol **146:** 1267–1281

Depuydt S, Trenkamp S, Fernie AR, Elftieh S, Renou J-P, Vuylsteke M, Holsters M, Vereecke D (2009) An integrated genomics approach to define niche establishment by *Rhodococcus fascians*. Plant Physiol **149:** 1366–1386

Desomer J, Dhaese P, Van Montagu M (1988) Conjugative transfer of cadmium resistance plasmids in *Rhodococcus fascians* strains. J Bacteriol **170:** 2401–2405

De Veylder L, Beeckman T, Beemster GTS, de Almeida Engler J, Ormenese S, Maes S, Naudts M, Van Der Schueren E, Jacqmard A, Engler G, et al (2002) Control of proliferation, endoreduplication and differentiation by the *Arabidopsis* E2Fa/DPa transcription factor. EMBO J **21:** 1360–1368

De Veylder L, Beeckman T, Beemster GTS, Krols L, Terras F, Landrieu I, Van Der Schueren E, Maes S, Naudts M, Inzé D (2001) Functional analysis of cyclin-dependent kinase inhibitors of *Arabidopsis*. Plant Cell **13:** 1653–1667

De Veylder L, Joubès J, Inzé D (2003) Plant cell cycle transitions. Curr Opin Plant Biol **6:** 536–543

Dewitte W, Murray JAH (2003) The plant cell cycle. Annu Rev Plant Biol **54:** 235–264

Dewitte W, Riou-Khamlichi C, Scofield S, Healy JMS, Jacqmard A, Kilby NJ, Murray JAH (2003) Altered cell cycle distribution, hyperplasia, and inhibited differentiation in *Arabidopsis* caused by the D-type cyclin CYCD3. Plant Cell **15:** 79–92

Dewitte W, Scofield S, Alcasabas AA, Maughan SC, Menges M, Braun N, Collins C, Nieuwland J, Prinsen E, Sundaresan V, et al (2007) *Arabidopsis* CYCD3 D-type cyclins link cell proliferation and endocycles and are rate-limiting for cytokinin responses. Proc Natl Acad Sci USA **104:** 14537–14542

Donnelly PM, Bonetta D, Tsukaya H, Dengler RE, Dengler NG (1999) Cell cycling and cell enlargement in developing leaves of *Arabidopsis*. Dev Biol **215:** 407–419

Ferjani A, Horiguchi G, Yano S, Tsukaya H (2007) Analysis of leaf development in *fugu* mutants of Arabidopsis reveals three compensation modes that modulate cell expansion in determinate organs. Plant Physiol **144:** 988–999

Francis D, Sorrell DA (2001) The interface between the cell cycle and plant growth regulators: a mini review. Plant Growth Regul **33:** 1–12

Galbraith DW, Harkins KR, Knapp S (1991) Systemic endopolyploidy in *Arabidopsis thaliana*. Plant Physiol **96:** 985–989

Gendreau E, Höfte H, Grandjean O, Brown S, Traas J (1998) Phytochrome controls the number of endoreduplication cycles in the *Arabidopsis thaliana* hypocotyl. Plant J **13:** 221–230

Gendreau E, Orbovic V, Höfte H, Traas J (1999) Gibberellin and ethylene control endoreduplication levels in the *Arabidopsis thaliana* hypocotyl. Planta **209:** 513–516

Goethals K, Vereecke D, Jaziri M, Van Montagu M, Holsters M (2001) Leafy gall formation by *Rhodococcus fascians*. Annu Rev Phytopathol **39:** 27–52

Hemerly A, de Almeida Engler J, Bergounioux C, Van Montagu M, Engler G, Inzé D, Ferreira P (1995) Dominant negative mutants of the Cdc2 kinase uncouple cell division from iterative plant development. EMBO J **14:** 3925–3936

Hu Y, Bao F, Li J (2000) Promotive effect of brassinosteroids on cell division involves a distinct *CycD3*-induction pathway in *Arabidopsis*. Plant J **24:** 693–701

Imai KK, Ohashi Y, Tsuge T, Yoshizumi T, Matsui M, Oka A, Aoyama T (2006) The A-type cyclin CYCA2;3 is a key regulator of ploidy levels in *Arabidopsis* endoreduplication. Plant Cell **18:** 382–396

Inzé D (2005) Green light for the cell cycle. EMBO J **24:** 657–662

Inzé D, De Veylder L (2006) Cell cycle regulation in plant development. Annu Rev Genet **40:** 77–105

Jasinski S, Riou-Khamlichi C, Roche O, Perennes C, Bergounioux C, Glab N (2002) The CDK inhibitor NtKIS1a is involved in plant development, endoreduplication and restores normal development of cyclin D3;1-overexpressing plants. J Cell Sci **115:** 973–982

Joubès J, Phan T-H, Just D, Rothan C, Bergounioux C, Raymond P, Chevalier C (1999) Molecular and biochemical characterization of the involvement of cyclin-dependent kinase A during the early development of tomato fruit. Plant Physiol **121:** 857–869

Kondorosi E, Kondorosi A (2004) Endoreduplication and activation of the anaphase-promoting complex during symbiotic cell development. FEBS Lett **567:** 152–157

Kosugi S, Ohashi Y (2003) Constitutive E2F expression in tobacco plants exhibits altered cell cycle control and morphological change in a cell type-specific manner. Plant Physiol **132:** 2012–2022

Lammens T, Boudolf V, Kheibarshekan L, Zalmas LP, Gaamouche T, Maes S, Vanstraelen M, Kondorosi E, La Thangue NB, Govaerts W, et al (2008) Atypical E2F activity restrains $APC/C^{CCS52A2}$ function obligatory for endocycle onset. Proc Natl Acad Sci USA **105:** 14721–14726

Laureys F, Dewitte W, Witters E, Van Montagu M, Inzé D, Van Onckelen H (1998) Zeatin is indispensable for the G_2-M transition in tobacco BY-2 cells. FEBS Lett **426:** 29–32

Leiva-Neto JT, Grafi G, Sabelli PA, Dante RA, Woo YM, Maddock S, Gordon-Kamm WJ, Larkins BA (2004) A dominant negative mutant of cyclin-dependent kinase A reduces endoreduplication but not cell size or gene expression in maize endosperm. Plant Cell **16:** 1854–1869

Livak KJ, Schmittgen TD (2001) Analysis of relative gene expression data using real-time quantitative PCR and the $2^{-\Delta\Delta C_T}$ method. Methods **25:** 402–408

Magyar Z, De Veylder L, Atanassova A, Bakó L, Inzé D, Bögre L (2005) The role of the *Arabidopsis* E2FB transcription factor in regulating auxin-dependent cell division. Plant Cell **17:** 2527–2541

Melaragno JE, Mehrotra B, Coleman AW (1993) Relationship between endopolyploidy and cell size in epidermal tissue of *Arabidopsis*. Plant Cell **5:** 1661–1668

Menges M, de Jager SM, Gruissem W, Murray JAH (2005) Global analysis of the core cell cycle regulators of Arabidopsis identifies novel genes, reveals multiple and highly specific profiles of expression and provides a coherent model for plant cell cycle control. Plant J **41:** 546–566

Menges M, Samland AK, Planchais S, Murray JAH (2006) The D-type cyclin CYCD3;1 is limiting for the G1-to-S-phase transition in *Arabidopsis*. Plant Cell **18:** 893–906

Nakai T, Kato K, Shinmyo A, Sekine M (2006) *Arabidopsis* KRPs have distinct inhibitory activity toward cyclin D2-associated kinases, including plant-specific B-type cyclin-dependent kinase. FEBS Lett **580:** 336–340

Nath U, Crawford BCW, Carpenter R, Coen E (2003) Genetic control of surface curvature. Science **299:** 1404–1407

Oakenfull EA, Riou-Khamlichi C, Murray JAH (2002) Plant D-type cyclins and the control of G1 progression. Philos Trans R Soc Lond B Biol Sci **357:** 749–760

Pertry I, Václavíková K, Depuydt S, Galuszka P, Spíchal L, Temmerman W, Stes E, Schmülling T, Kakimoto T, Van Montagu M, et al (2009) Identification of *Rhodococcus fascians* cytokinins and their modus operandi to reshape the plant. Proc Natl Acad Sci USA **106:** 929–934

Pettkó-Szandtner A, Mészáros T, Horváth GV, Bakó L, Csordás-Tóth É, Blastyák A, Zhiponova M, Miskolczi P, Dudits D (2006) Activation of an alfalfa cyclin-dependent kinase inhibitor by calmodulin-like domain protein kinase. Plant J **46:** 111–123

Putnam ML, Miller ML (2007) *Rhodococcus fascians* in herbaceous perennials. Plant Dis **91:** 1064–1076

Riou-Khamlichi C, Huntley R, Jacqmard A, Murray JAH (1999) Cytokinin activation of *Arabidopsis* cell division through a D-type cyclin. Science **283:** 1541–1544

Riou-Khamlichi C, Menges M, Healy JMS, Murray JAH (2000) Sugar control of the plant cell cycle: differential regulation of *Arabidopsis* D-type cyclin gene expression. Mol Cell Biol **20:** 4513–4521

Schnittger A, Schöbinger U, Bouyer D, Weinl C, Stierhof Y-D, Hülskamp M (2002) Ectopic D-type cyclin expression induces not only DNA

replication but also cell division in *Arabidopsis* trichomes. Proc Natl Acad Sci USA **99:** 6410–6415

Schnittger A, Weinl C, Bouyer D, Schöbinger U, Hülskamp M (2003) Misexpression of the cyclin-dependent kinase inhibitor *ICK1/KRP1* in single-celled *Arabidopsis* trichomes reduces endoreduplication and cell size and induces cell death. Plant Cell **15:** 303–315

Simón-Mateo C, Depuydt S, de Oliveira Manes CL, Cnudde F, Holsters M, Goethals K, Vereecke D (2006) The phytopathogen *Rhodococcus fascians* breaks apical dominance and activates axillary meristems by inducing plant genes involved in hormone metabolism. Mol Plant Pathol **7:** 103–112

Soni R, Carmichael JP, Shah ZH, Murray JAH (1995) A family of cyclin D homologs from plants differentially controlled by growth regulators and containing the conserved retinoblastoma protein interaction motif. Plant Cell **7:** 85–103

Sorrell DA, Combettes B, Chaubet-Gigot N, Gigot C, Murray JAH (1999) Distinct cyclin D genes show mitotic accumulation or constant levels of transcripts in tobacco Bright Yellow-2 cells. Plant Physiol **119:** 343–351

Spíchal L, Kryštof V, Paprskářová Lenobel R, Stýskala J, Binarová P, Cenklová V, De Veylder L, Inzé D, Kontopidis G, Fischer PM, et al (2007) Classical anticytokinins do not interact with cytokinin receptors but inhibit cyclin-dependent kinases. J Biol Chem **282:** 14356–14363

Stals H, Inzé D (2001) When plant cells decide to divide. Trends Plant Sci **6:** 359–364

Temmerman W, Vereecke D, Dreesen R, Van Montagu M, Holsters M, Goethals K (2000) Leafy gall formation is controlled by *fasR*, an AraC-type regulatory gene, in *Rhodococcus fascians*. J Bacteriol **182:** 5832–5840

Traas J, Hülskamp M, Gendreau E, Höfte H (1998) Endoreduplication and development: rule without dividing? Curr Opin Plant Biol **1:** 498–503

Tsukaya H (2006) Mechanism of leaf-shape determination. Annu Rev Plant Biol **57:** 477–496

Vandeputte O, Öden S, Mol A, Vereecke D, Goethals K, El Jaziri M, Prinsen E (2005) Biosynthesis of auxin by the Gram-positive phytopathogen *Rhodococcus fascians* is controlled by compounds specific to infected plant tissues. Appl Environ Microbiol **71:** 1169–1177

Vandeputte O, Vereecke D, Mol A, Lenjou M, Van Bockstaele D, El Jaziri M, Baucher M (2007) *Rhodococcus fascians* infection accelerates progression of tobacco BY-2 cells into mitosis through rapid changes in plant gene expression. New Phytol **175:** 140–154

Vereecke D, Burssens S, Simón-Mateo C, Inzé D, Van Montagu M, Goethals K, Jaziri M (2000) The *Rhodococcus fascians*-plant interaction: morphological traits and biotechnological applications. Planta **210:** 241–251

Vereecke D, Cornelis K, Temmerman W, Holsters M, Goethals K (2002a) Versatile persistence pathways for pathogens of animals and plants. Trends Microbiol **10:** 485–488

Vereecke D, Cornelis K, Temmerman W, Jaziri M, Van Montagu M, Holsters M, Goethals K (2002b) Chromosomal locus that affects the pathogenicity of *Rhodococcus fascians*. J Bacteriol **184:** 1112–1120

Verkest A, de O Manes C-L, Vercruysse S, Maes S, Van Der Schueren E, Beeckman T, Genschik P, Kuiper M, Inzé D, De Veylder L (2005) The cyclin-dependent kinase inhibitor KRP2 controls the onset of the endoreduplication cycle during *Arabidopsis* leaf development through inhibition of mitotic CDKA;1 kinase complexes. Plant Cell **17:** 1723–1736

Vlieghe K, Boudolf V, Beemster GTS, Maes S, Magyar Z, Atanassova A, de Almeida Engler J, De Groodt R, Inzé D, De Veylder L (2005) The DP-E2F-like *DEL1* gene controls the endocycle in *Arabidopsis thaliana*. Curr Biol **15:** 59–63

Wang H, Qi Q, Schorr P, Cutler AJ, Crosby WL, Fowke LC (1998) ICK1, a cyclin-dependent protein kinase inhibitor from *Arabidopsis thaliana* interacts with both Cdc2a and CycD3, and its expression is induced by abscisic acid. Plant J **15:** 501–510

Weinl C, Marquardt S, Kuijt SJH, Nowack MK, Jakoby MJ, Hülskamp M, Schnittger A (2005) Novel functions of plant cyclin-dependent kinase inhibitors, ICK1/KRP1, can act non-cell-autonomously and inhibit entry into mitosis. Plant Cell **17:** 1704–1722

Zhang K, Diederich L, John PCI (2005) The cytokinin requirement for cell division in cultured *Nicotiana plumbaginifolia* cells can be satisfied by yeast Cdc25 protein tyrosine phosphatase: implications for mechanisms of cytokinin response and plant development. Plant Physiol **137:** 308–316

Zhang Y, Wang Z, Ravid K (1996) The cell cycle in polyploid megakaryocytes is associated with reduced activity of cyclin B1-dependent Cdc2 kinase. J Biol Chem **271:** 4266–4272